

Self-Assembly Kinetics of Amphiphilic Dendritic Copolymers

*Cuiyun Zhang¹²³, You Fan⁵, Yunyi Zhang¹²³, Cong Yu^{*23}, Hongfei Li^{*34}, Yu Chen^{*5},
Ian W. Hamley^{*6}, Shichun Jiang^{*1}*

¹School of Materials Science and Engineering, Tianjin University, Tianjin 300072, P.
R. China

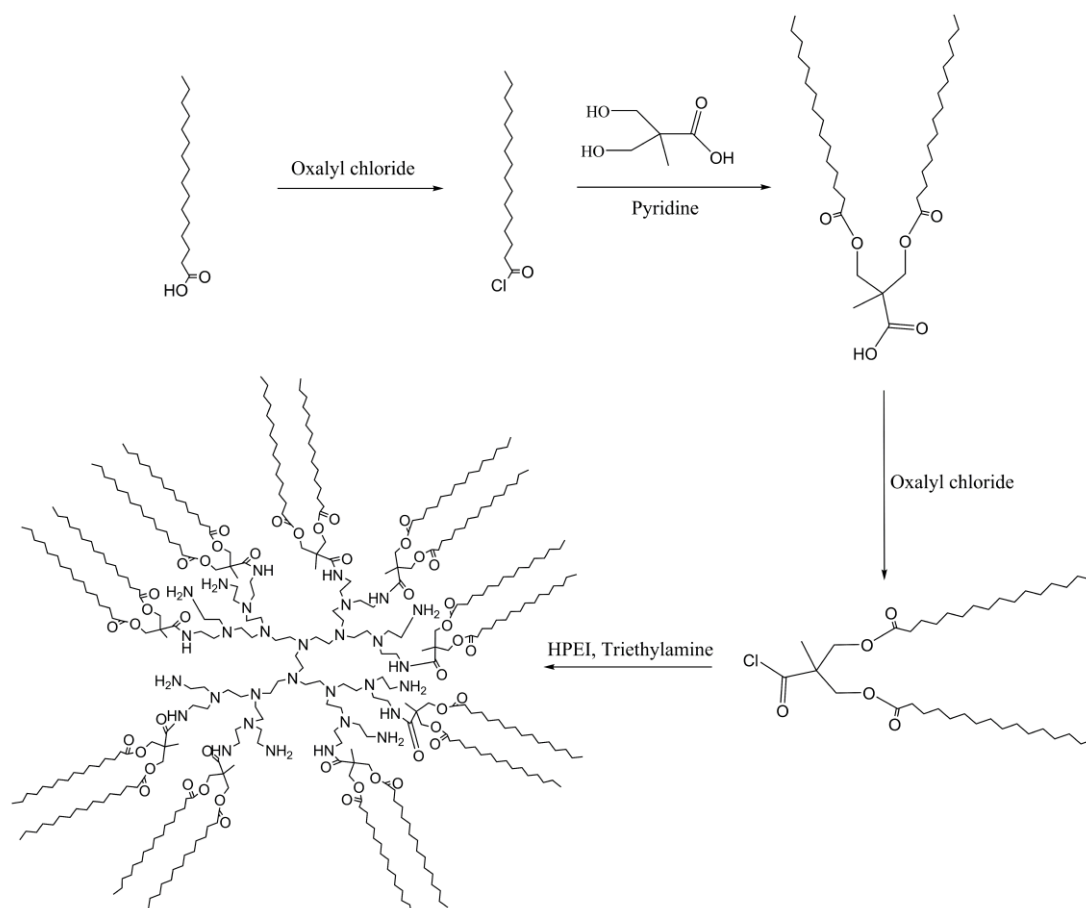
²State Key Laboratory of Electroanalytical Chemistry, Changchun Institute of Applied
Chemistry, Chinese Academy of Sciences, Changchun 130022, P. R. China

³University of Chinese Academy of Science, Beijing, 100049, P. R. China

⁴State Key Laboratory of Polymer Physics and Chemistry, Changchun Institute of
Applied Chemistry, Chinese Academy of Sciences, Changchun 130022, P. R. China

⁵Department of Chemistry, School of Sciences, Tianjin University, Tianjin 300072, P.
R. China

⁶School of Chemistry, Pharmacy and Food Biosciences, University of Reading,
Whiteknights, Reading RG6 6AD, United Kingdom



Scheme S1. Synthesis of amphiphilic dendritic copolymers with a hydrophilic HPEI core and a hydrophobic shell.

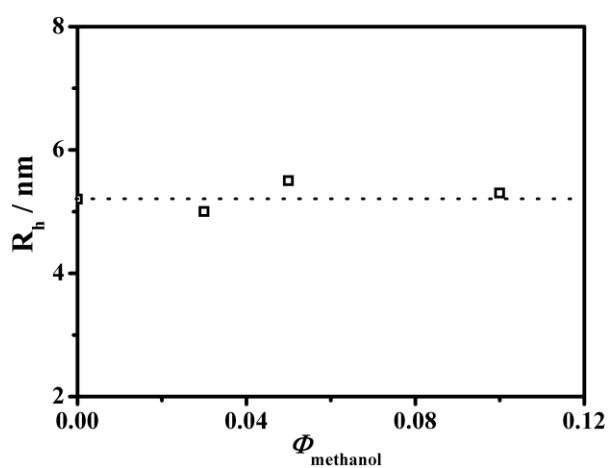


Figure S1. Variation of the hydrodynamic radius of P-1 with increasing volume fraction of methanol.

The self-assembly morphologies of the ADPs were characterized by a high resolution transmission electron microscope (TEM, JEM-2100F, Philips, The

Netherlands) operating at an acceleration voltage of 200 kV. The sample solution was deposited onto a carbon-coated copper grid and then the excess solution was blotted away using a strip of filter paper. The samples were dried at room temperature for one day prior to observation. The morphology of the micelles is influenced by the evaporation of the solvent. In this experiment, for P-1 and P-2 10 μ L solution was deposited onto the copper grid and for P-3 and P-4 30 μ L solution was deposited onto the copper grid. If more than 30 μ L solution is deposited onto the copper grid, the micelles will fuse to form large micelles. The morphology of the micelles formed by P-1, P-2, P-3 and P-4 is shown in Fig.7. The radii of the micelles observed by TEM are 39 nm, 33 nm, 28 nm and 19 nm for P-1, P-2, P-3, and P-4. The values of R_g obtained from the Guinier plot are 37 nm, 34 nm, 30 nm, 20 nm. The size of the micelles observed by TEM is consistent with the results from the Guinier plot.

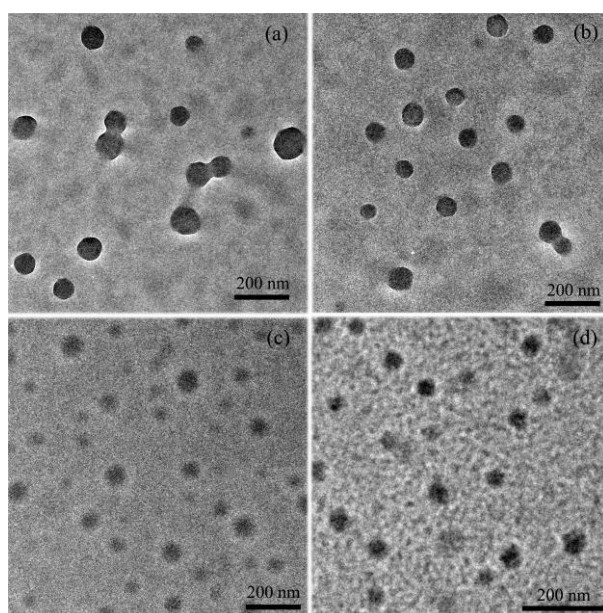


Figure S2. TEM images of the micelles of P-1 (a), P-2 (b), P-3 (c), and P-4 (d) at CMC.

Influence of polydispersity on the self-assembly

The polydispersity of the ADPs results from the hyperbranched core and the branched shell. Yan reported that with the increasing degree of branching of the core the amphiphilic hyperbranched multiarm copolymers self-assembled into vesicles, wormlike micelles, and spherical micelles.¹ In this study, the $f_{\text{shell/core}}$ changes from 5.2 to 8.3 (Table 1) and the self-assembly morphology is micelle in this ratio range. For the amphiphilic block copolymer with polydisperse distribution of the hydrophilic part, the segregation of polymer chains cause the change of vesicle size and phase boundaries.² Because there is no phase separation for the ADPs, the self-assembly morphology is not influenced by the polydispersity of the core and shell. At the same concentration, with a higher DA, the micelles have larger R_h (Figure 12 b), indicating that the major influence of the polydispersity on the self-assembly of the ADPs is the micelle size. For the thermosensitive diblock copolymers, the distribution of R_h becomes broader with the increasing polydispersity of the thermosensitive part.³ Also, block copolymers with high polydispersity form polydisperse vesicles due to the segregation of the polymer chains.⁴ However, as shown in Figure 8, the PDI of the hydrodynamic radius distribution is relatively narrow (< 0.16). The count rate, hydrodynamic radius and relaxation time in this study are average values. The self-assembly mechanism agrees well with the computer simulation in which the amphiphilic hyperbranched copolymer is monodisperse.⁵ The conclusion in this study is not influenced by the polydispersity.

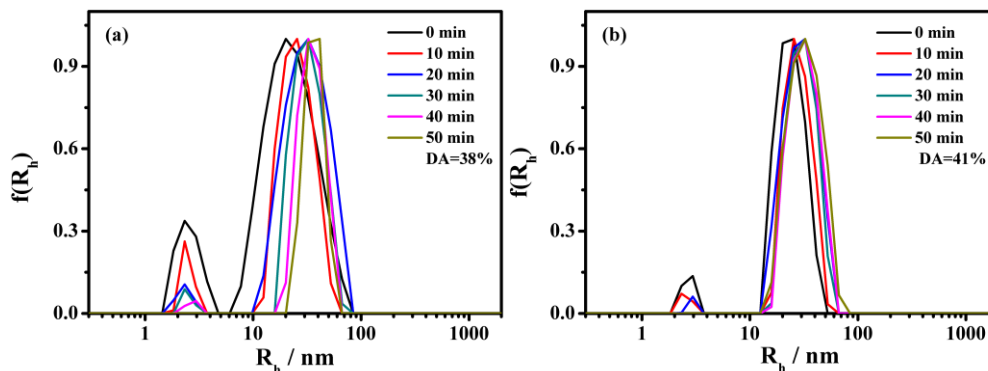


Figure S3. The distribution functions of the apparent hydrodynamic radius of P-1, P-2 at CMC.

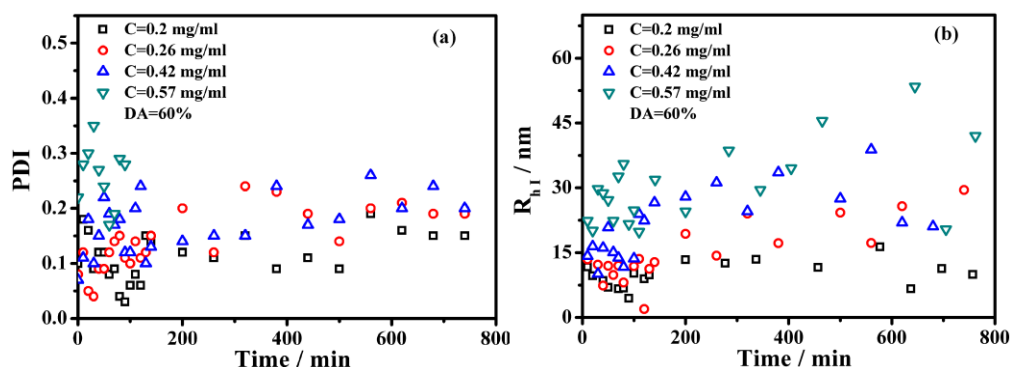


Figure S4. The polydispersity index and the increased hydrodynamic radius as a function of time at different concentration for P-4.

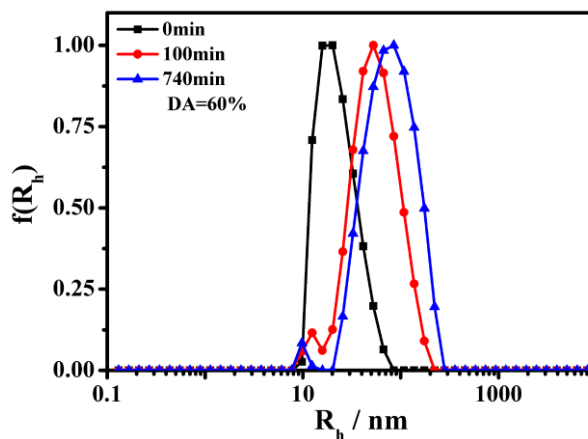


Figure S5. Variation of the distribution of hydrodynamic radius with time for P-4 at 0.57 mg/mL.

The hydrodynamic radius of P-4 is 7.3 nm. The small peak is the dimers or trimers of the ADPs. For the giant vesicles, the fission of mother vesicles will give birth to daughter vesicles.⁶ Some unstable big micelles may form at the concentration higher

than CMC. As shown in Figure 7, at the CMC the values of R_{h1} are smaller than the size of the smallest micelles in the distribution of R_h , indicating that the growing of micelles is due to the fission and fusion between the big micelles. At the concentration higher than CMC, the values of R_{h1} are larger than the size of the smallest micelles in the distribution of R_h , indicating that both fusion of the small micelles with big micelles and fission and fusion between the big micelles will happen. Compared with the linear block copolymers, the lacking of phase separation for the ADPs makes the fission of big micelles easier. In the process of approaching equilibrium, the fission of unstable big micelle gives birth to small micelles (dimers or trimers). Compared with the unimers, the dimmers and trimmers are relatively more stable. Since the concentration of dimmers or trimers is not large in comparison with that of micelles having an average size, the collision probability will be small and the dimmers or trimmers will exist for a relatively long time.⁷ Thus, in the distribution of the hydrodynamic radius the small peak corresponding to the dimers or trimmers is observed.

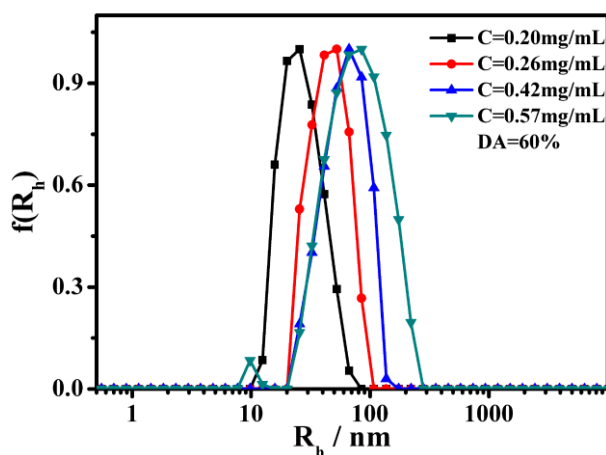


Figure S6. Variation of the distribution of the hydrodynamic radius with concentration at 740 min.

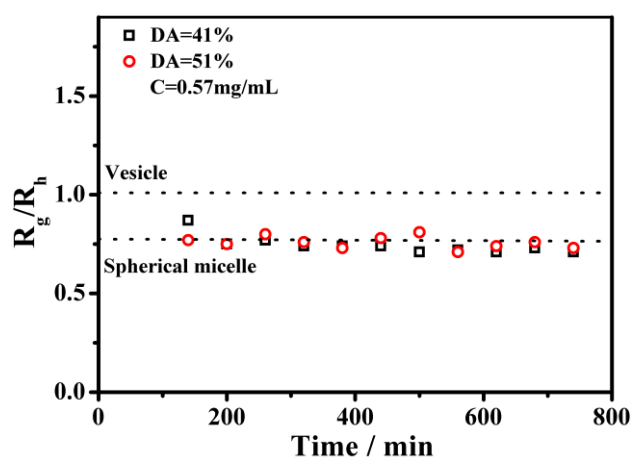


Figure S7. The ratio of R_g and R_h as a function of the time for P-2, P-4.

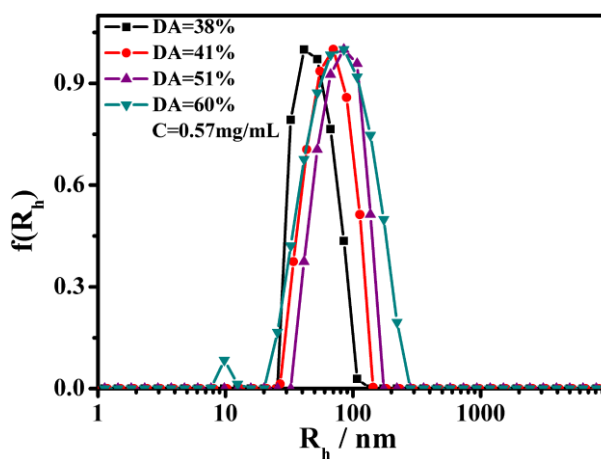


Figure S8. The variation of the distribution of the hydrodynamic radius with DA at 0.57 mg/mL.

REFERENCES

1. Cheng, H.; Yuan, X.; Sun, X.; Li, K.; Zhou, Y.; Yan, D. Effect of Degree of Branching on the Self-Assembly of Amphiphilic Hyperbranched Multiarm Copolymers. *Macromolecules* **2010**, *43*, 1143-1147.
2. Terreau, O.; Luo, L.; Eisenberg, A. Effect of Poly(acrylic acid) Block Length Distribution on Polystyrene-*b*-Poly(acrylic acid) Aggregates in Solution. 1. Vesicles. *Langmuir* **2003**, *19*, 5601-5607.
3. Seno, K. I.; Kanaoka, S.; Aoshima, S. Thermosensitive Diblock Copolymers with

- Designed Molecular Weight Distribution: Synthesis by Continuous Living Cationic Polymerization and Micellization Behavior. *J. Polym. Sci., Part A: Polym. Chem.* **2008**, 46, 2212-2221.
4. Terreau, O.; Bartels, C.; Eisenberg, A. Effect of Poly(acrylic acid) Block Length Distribution on Polystyrene-*b*-poly(acrylic acid) Block Copolymer Aggregates in Solution. 2. A Partial Phase Diagram. *Langmuir* **2004**, 20, 637-645.
5. Wang, Y.; Li, B.; Zhou, Y.; Lu, Z.; Yan, D. Dissipative Particle Dynamics Simulation Study on the Mechanisms of Self-assembly of Large Multimolecular Micelles from Amphiphilic Dendritic Multiarm Copolymers. *Soft Matter* **2013**, 9, 3293-3304.
6. Zhou, Y.; Yan, D. Real-Time Membrane Fission of Giant Polymer Vesicles. *Angew. Chem. Int. Ed.* **2005**, 44, 3223-3226.
7. Esselink, F. J.; Dormidontova, E.; Hadziioannou, G. Evolution of Block Copolymer Micellar Size and Structure Evidenced with Cryo Electron Microscopy. *Macromolecules* **1998**, 31, 2925-2932.